DIRAC 2001-02
March 14, 2001

Muon identification in DIRAC experiment

V. Brekhovskikh[♯], M. V. Gallas[♭]
[♯] Protvino IHEP, [♭] CERN

Abstract

The μ-identification problem in DIRAC spectrometer is studied. Description and results of muon finder procedure are shown and the needed input-output variables established. As a result of these studies some "experimental" constants should be added to detector.dat file in order to get a better description of muon detector placement by correction of survey geometry data. Acceptable time and spatial coordinates cuts for "muon-signal" definition are also proposed. Finally some physical consequences of muon extraction are presented.

The goal of μ-identification in DIRAC experiment [1] is to clean the $\pi^+\pi^-$ trigger data sample and remove those events in which a muon instead of a pion is detected. Of course, the way to do this is a selective way; this means that muon label is associated to reconstructed tracks and the events should be accepted as good $\pi^+\pi^-$ if there are at least two tracks (positive and negative) without muon label. Events with multiplicity higher than $1+1$ can be saved even though there is a muon signal for one of these tracks. This and the off-line definition of "muon signal" are the advantages of the off-line muon subtraction with respect to an on-line muon trigger used as a veto.

For μ-identification purpose a muon detector (*Mu*) was installed at the end of DIRAC two arm spectrometer. Two scintillation counter layers per arm, behind iron absorber, and the associated electronics (CFD+Meantimer+TDC) detect muons from pion decays that cross the iron absorber. Apart from *Mu* data, preshower detector (*Prsh*) could also help in the muon track identification. Because there is no way to reconstruct tracks after drift chambers (*DC*), *Prsh* detector must be used to ensure that the particle associated with a reconstructed track reaches the iron absorber. After that if a muon hit is detected in proper spatial, x, and time, t, coordinates the muon nature of the reconstructed track is feasible [1]

Muon and preshower data were not used at all during the 1999 data-processing and for the 2000 data-processing the raw data should be prepared. Preshower data come from the 16 individual ADC-channels and 16 time-channels; amplitude and time alignment is not done for 2000-data although these data can be used to check that hit in the expected preshower slab is present; further constraints in ADC and time information are not possible unless data will be prepared. The muon time alignment was performed for a subset of

[1]The iron absorber for muon detector was designed in order to minimize the admixture of muons in pion data and the rejected pions, identified like muons, are around $2-3\%$ (V.Yazkov, private communication).

2000-data [2] and this allows us to use time criteria (base on a good time resolution of *Mu* detector) in parallel with x-coordinate criteria to define "muon-signal". Concerning to 1999-data the muon identification is hard because at that run period the muon detector suffered from a huge background and the collected data came not from TDC but from registers L2366 (two muon-slabs per channel). Only in 2000 year, after introduction of second muon layer, meantimer and TDC electronics [2], it is possible to make a reasonable muon identification for which the preliminary results[3] showed a 10% reduction of the initial $\pi^+\pi^-$ trigger data sample after subtraction of $\mu\pi$, $\pi\mu$, and $\mu\mu$ events.

1 The muon finder procedure

The way to identify muon tracks has the following *steps*:

- For each reconstructed track at the level of DC chambers it is needed to extrapolate it to the z-coordinate of *Prsh* and *Mu* detector planes and obtain the coordinates (x', y', z') of the track intersection point with these detector planes in local reference system given by *MoPlanesToTLN* ARIANE subroutine.

- After this, the procedure should scan over all muon hits ("good time" information is required) looking for a hit slab in the appropriate spectrometer arm and center slab position, $x'_{centerslab}$, "close enough" to the coordinate of track intersection point[3], x'_{tr} . Of course the studied track should be in the acceptance of *Prsh* and *Mu* detectors.

- Once a muon hit is associated with a track, *Prsh* information could also be used to ensure that at least the particle reached the iron absorber and the muon hit slab was not originated by a coincidence of a DC track and background hit coming from the downstream wall. To use *Prsh* it is needed to follow the same strategy as used in the previous step.

Input data to *PrshMuFinder(XyzTr,IsaMuon)* subroutine are the (x, y, z) coordinates of two points of a DC-track in secondary reference system. The real input array $XyzTr(3, 2)$ is enough to establish arm and muon characteristic of the track. As an example one can use $ParTrDC(3, 2, nTr, nArm)$ variables from $TmTrxDC$ common block as input data. The *output* is given by the integer vector *IsaMuon(2)* in which the first number is the muon hit slab associated with the track defined by $XyzTr(3, 2)$ and the second number corresponds to the Prsh hit slab. Internally, the *PrshMuFinder(XyzTr,IsaMuon)* calls to *MuFinder(XyzTr,FoundHitSlabMu)* and PrshFinder(XyzTr,FoundHitSlabPrsh) subroutines to find the hit-track correspondence in *Mu* and *Prsh* detectors, in this way they can be used independently for other purposes in ARIANE. The output variables: *FoundHitSlabPrsh, FoundHitSlabMu and IsaMuon(2)* can be 0, positive or negative integer numbers. The 0 value means that was not found any time hit in the arm corresponding to the analyzed track. Positive numbers correspond to the number of slab hit by the track. Negative

[2]The analysis presented in this report is based on ~ 35 million events of mix-trigger 2000-data from run number 2454 to 2523.

[3]"good time" information and "close enough" x-coordinate are concepts that will be defined latter and will be adjustable by the users

numbers could appear if there is a time hit in the apropriatte arm but time and spatial criteria are not satisfied and then the hit does not match with the track.

As has been mentioned, the muon finder procedure involves cuts in time and x' coordinate to define "muon signal" and reject "muon background" hits. These cuts will be made available to the muon finder procedure through the appropriate *FFreadInput* cards: *DtwindowMusignal* and *DxwindowMusignal*. After muon time alignment the user can define a window $[-DtwindowMusignal, DtwindowMusignal]$ in such a way that time of "muon signal" must be in this interval. In a similar manner it is possible to play with x'_{tr} coordinate and define "muon signal" only if $|x'_{center\,slab} - x'_{tr}| \leq DxwindowMusignal$; but $DxwindowMusignal$ can not be half of muon slab width due to huge multiple scattering inside iron absorber.

Multiple scattering and tracks that cross two slabs in *Prsh* have been also introduced in the muon finder algorithm. In those situations in which the track hit a *Prsh* slab in a slice of $xslicePrsh\,cm$ next to slab edge and time information was not found in this slab the algorithm looks for a hit in the appropriate adjacent slab. The variable $xslicePrsh$ will be made also available through FFreadInput card and the value $xslicePrsh = 3\,cm$ is enough to remove the Prsh-slab granularity in (x'_{tr}, y'_{tr}) coordinates projection at *Mu z* plane (see figure 12).

2 Muon data

2.1 Muon time alignment

For a subset ($\sim$ up to 2550) of 2000-runs a time alignment of 28×2 TDC L3377 time data channels was done. As a result all the *Mu*-time channels are now centered at zero and this means that particles with time zero are "in time" with the corresponding hit in vertical hodoscopes (*VH*).

Individual slab time hit distributions can be fitted to a gaussian and uniform background; the sigma per slab plotted for each muon arm as is shown in figures 1 and 2.

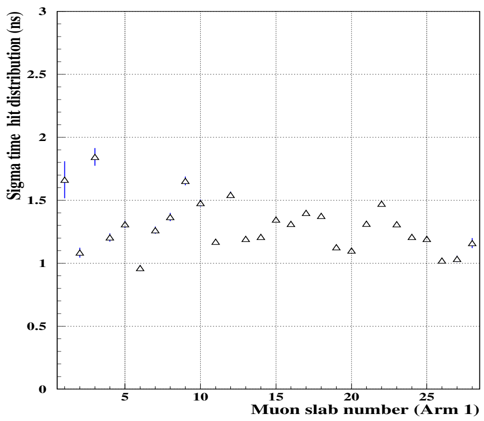

Figure 1: *Sigma of time hit distribution per muon slab in arm one after alignment procedure.*

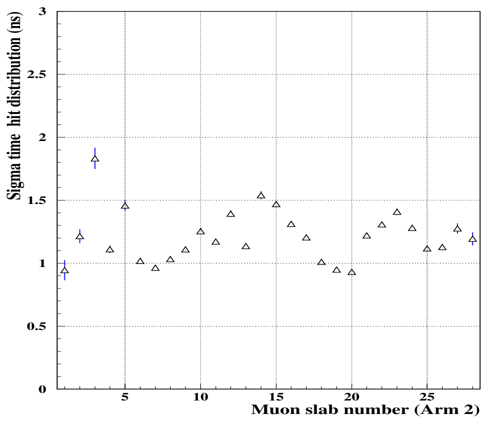

Figure 2: *Sigma of time hit distribution per muon slab in arm two after alignment procedure.*

Apart from the not clear slab structure, all slabs have a more or less acceptable time resolution (intrinsic TDC resolution is 0.5 ns).

The overall time resolution and background contamination can be extracted from the figures 3 and 4, individual slab time hit distributions were added and fitted to a gaussian plus a uniform background. The baseline spurious hits could contribute to a "false muon" identification in a proportion less than 1.5% for Arm1 and 2% for Arm 2 in the interval $[-5, +5]\,ns$. The non gaussian part of the distribution can be cut if we set $DtwindowMusignal = 4.0\,ns$ instead of $DtwindowMusignal = 5.0\,ns$.

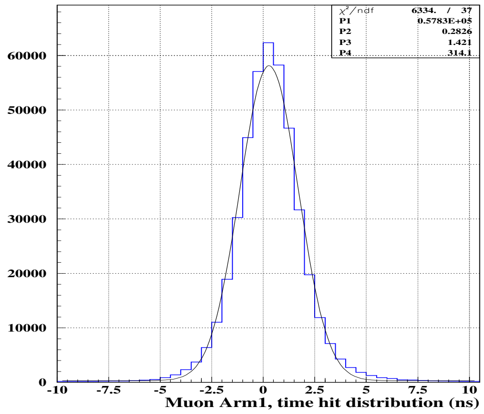

Figure 3: *Global time hit distribution in Arm1 Mu detector, after alignment procedure.*

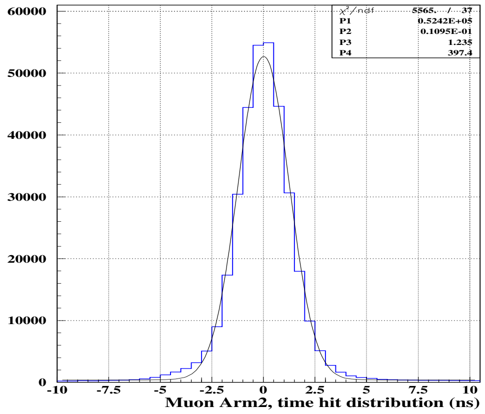

Figure 4: *Global time hit distribution in Arm2 Mu detector, after alignment procedure.*

2.2 Muon slabs placement and multiple scattering effect

Particle trajectories in muon iron absorber are strongly affected by multiple scattering. Iron thickness[4] from $60\,cm$ up to $140\,cm$, to take in account the momenta spectra from $1\,GeV/c$ up to $6\,GeV/c$, is responsible of a x'_{tr} coordinate large spread with respect to the hit slab center position $x'_{centerslab}$. Starting from $1+1$ track reconstructed events with only one "good time" muon hit per arm, $(x'_{tr} - x'_{centerslab})$ hit slab distribution shows the multiple scattering effect and eventually disagreements between $x'_{centerslab}$ values and experimental observed $(x'^{exp}_{centerslab})$ center slab positions.

Original distributions presented in figures 5 and 6 were not centered at zero, and $x'_{centerslab}$ detector.dat values have been corrected to $x'^{exp}_{centerslab}$ by use of x'_{tr} distribution per hit muon slab and large muon data statistics (subsection 2.2.1).

Apart form the edge effects in slabs 1 and 28 of both arms the two significant points are the individual baseline contamination which represents around 3% "false muon" identification and the widths of distributions. The shape of these distributions results from the slab width and multiple scattering effect with strong dominance of the latter. Sigma as function of slab is plotted in figure 7. Even though the iron absorber was designed to receive more or less the same answer for all momenta spectra there is an x' dependence and

[4] *Mu* absorber was build with iron blocks of thickness: $60, 80, 100, 125, 140\,cm$ and respective x'-widths of $80.5, 80, 60, 80, 60.5\,cm$.

it is possible to observe some trends related with iron thickness. These steps coincide with Mu slabs numbers $6, 13, 18, 25$, and are also visible in the Mu hit distributions (figure 10).

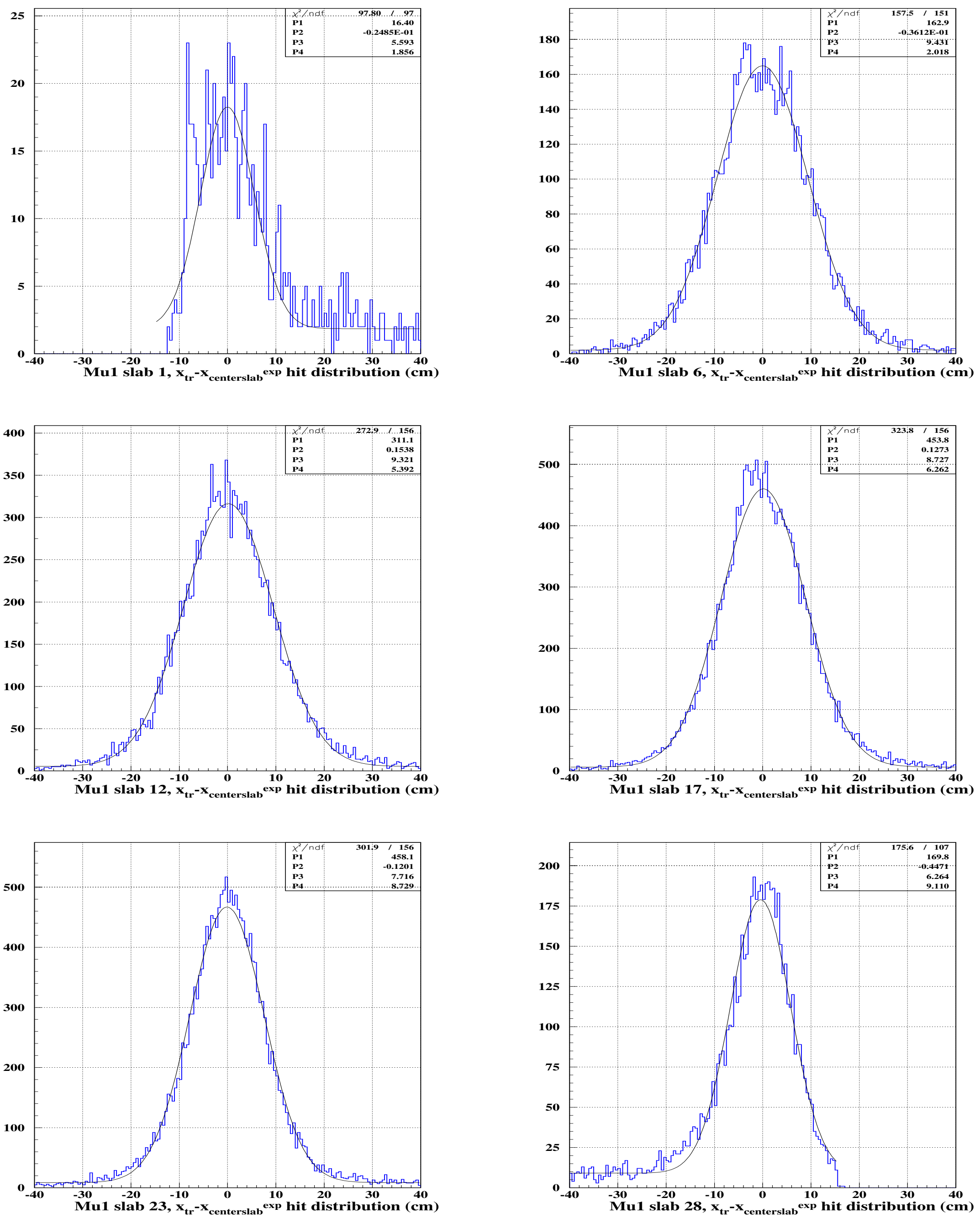

Figure 5: $(x'_{tr} - x'^{exp}_{centerslab})$ *distributions for muon Arm1 slabs:* $1, 6, 12, 17, 23, 28$. *Notation: P1 = gaussian cte, P2 = gaussian mean value, P3 = gaussian sigma, P4= uniform level.*

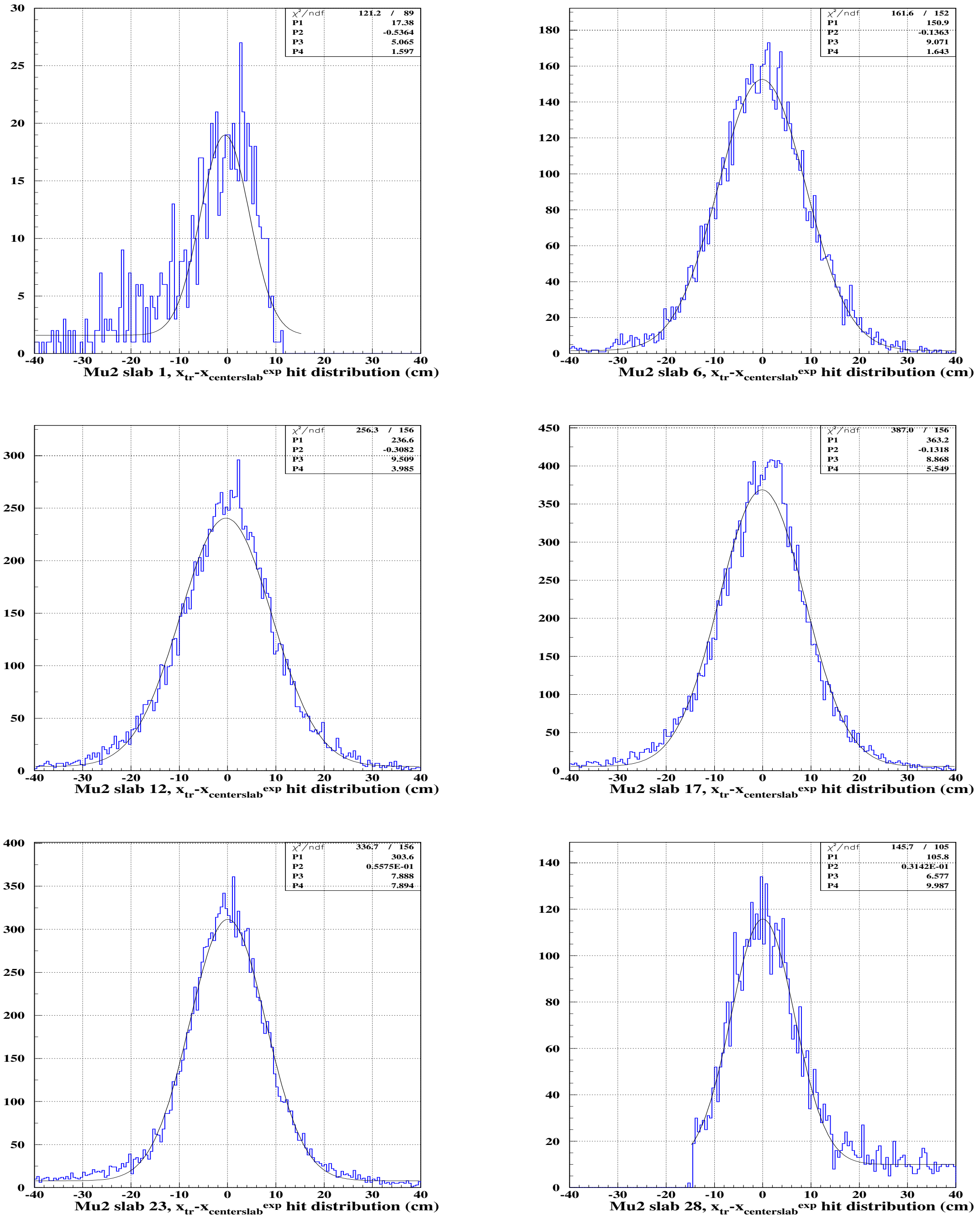

Figure 6: $(x'_{tr} - x'^{exp}_{centerslab})$ *distributions for muon Arm2 slabs:* $1, 6, 12, 17, 23, 28$. *Notation: P1 = gaussian cte, P2 = gaussian mean value, P3 = gaussian sigma, P4= uniform level.*

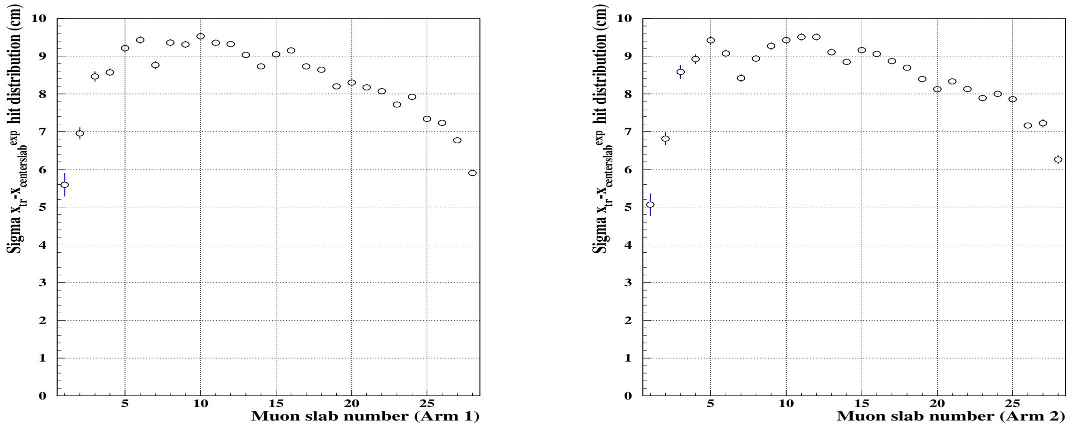

Figure 7: $(x'_{tr} - x'^{exp}_{centerslab})$ *sigma distributions per Mu slab, Arm1 and Arm2.*

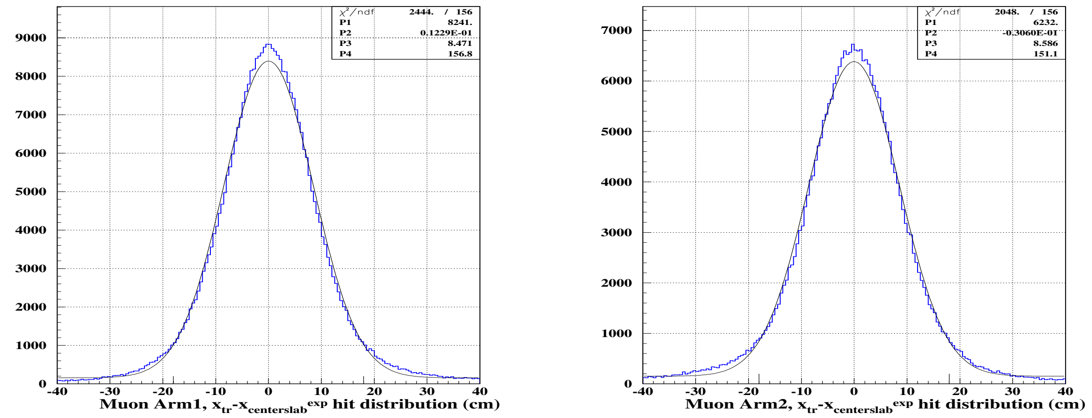

Figure 8: $(x'_{tr} - x'^{exp}_{centerslab})$ *distributions for all Mu slabs in Arm1 and Arm2. Notation: P1 = gaussian cte, P2 = gaussian mean value, P3 = gaussian sigma, P4= uniform level.*

As in case of t coordinate, adding these individual slab distributions is possible to extract the global base line contamination and them the proportion of "false muons". Figure 8 shows this contamination after fit to a gaussian plus a uniform level. The contamination can be estimated in $< 3\%$ for Arm1 and $< 4\%$ for Arm2 for the region $[-18, 18]\,cm$. The proposed x'-coordinate cut, $DxwindowMusignal = 18\,\text{cm}$, means in a practical sense that we mark as muons those events in which a muon hit was found in predicted slab by track procedure or adjacent one; and this is equivalent to a 2-σ cut in the distributions showed in figure 8. The reject part $|(x'_{tr} - x'^{exp}_{centerslab}| > 18\,cm$ is $\sim 8\%$ of the distributions and in this part the relation baseline contamination to muon signal is $1:1$.

2.2.1 Muon slabs placement

Apart from the time, muon alignment data was also needed to correct geometrical data in *detector.dat* in order to describe better the *Mu* center slab position. From a data sample of "good pair"events with $1 + 1$ tracks and only one Mu hit per arm, the x'_{tr} coordinate distribution per hit slab was fitted to a gaussian and the mean value taken as a center hit slab position. The differences $x'^{exp}_{centerslab} - x'_{centerslab}$ will be stored in the new *detector.dat* file, where $x'_{centerslab}$ values are stored by mean of x'_{slab1} and pitch of *Mu* detector ($12.1\,cm$). Experimental values are displayed in figure 9.

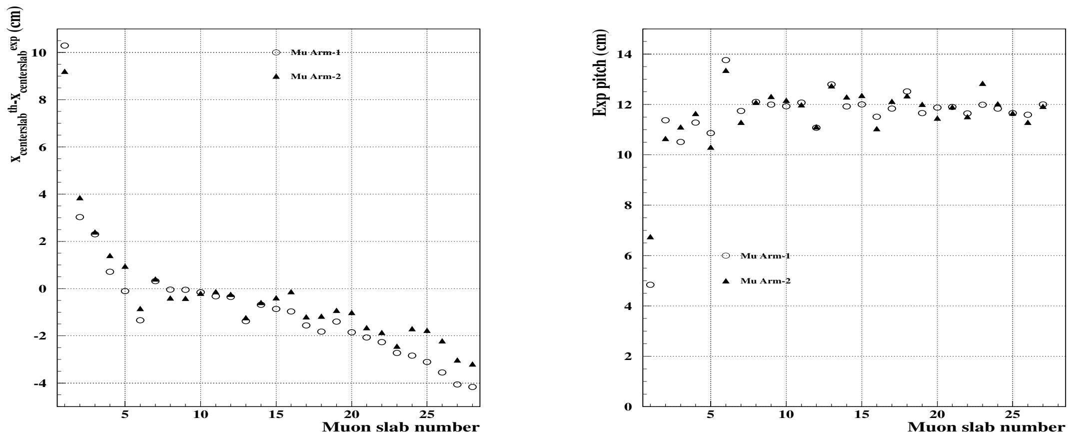

Figure 9: *Differences* $x'^{exp}_{centerslab} - x'_{centerslab}$ *and experimental pitch values for all Mu slabs.*

Another improvement that should be included in *detector.dat* concerns the *Mu* sensitive area. *Mu* sensitive area was slightly increased in the x' direction to take in account the multiple scattering effect ($3.92\,cm$ in the outer part and $5.12\,cm$ in the inner side).

3 Preshower data

Prsh data was not used for the present $A_{2\pi}$-data processing and the ADC and TDC information still remains as pure raw data. This data could induce a better muon identification so far amplitude and time are not aligned, *Prsh* comes to muon finder procedure in a soft way: only a presence of a time hit in proper slab is checked, no matter if time and amplitude are good. To outline two problems that should be also investigated: *Prsh* exhibits a central y' coordinate inefficiency probably due to Cherenkov (*Ch*) internal support and the amplitude spectra for pions shows a long tail compatible with electron signal.

4 Some results and physical considerations

As has been mentioned in section 2.2 the step thickness in iron absorber is visible in *Mu* hit distributions. Figure 10 shows *Mu* hit distributions for raw-data (crosses) and μ-candidates (solid line) by *PrshMuFinder* routine. The ratio between both informs about the "muon background" that was removed by muon finder procedure; inner and outer muon slabs are the most affected. Five trends limited by slabs $6, 13, 18, 25$ are present in *Mu* hit distributions and coincide with different thicknesses of iron absorber. This point should be taken into account in the on-line tuning job of *Mu* detector.

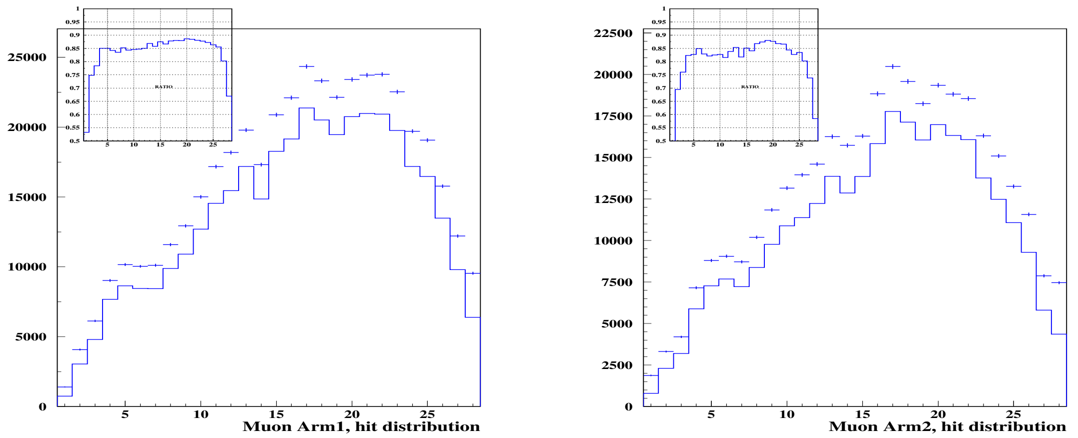

Figure 10: *Mu hit distributions for raw-data (crosses) and μ-candidates. Ratio between both is also displayed.*

Time, t, and x' coordinates criteria to define "muon signal", already reported, can be seen in figure 11

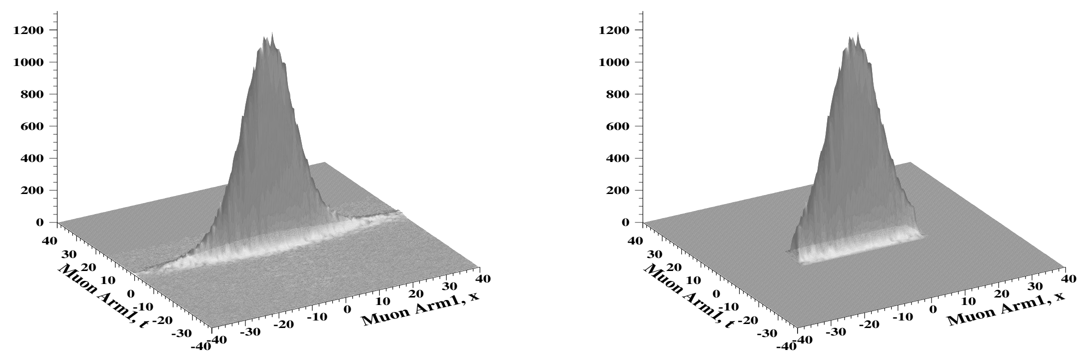

Figure 11: *Mu* $(x'_{tr} - x'^{exp}_{centerslab})$ *vs* t *distributions for aligned Mu data (left) and μ-candidates (right).*

Requirement on *Prsh* information does not produce undesired granularity effects in $x'\,vs\,y'$ scatter-plots for reconstructed tracks before and after muon finder procedure (figure12). This was achieved after taking into account the possible multiple scattering and tracks that cross two slabs in *Prsh* detector (see section 1).

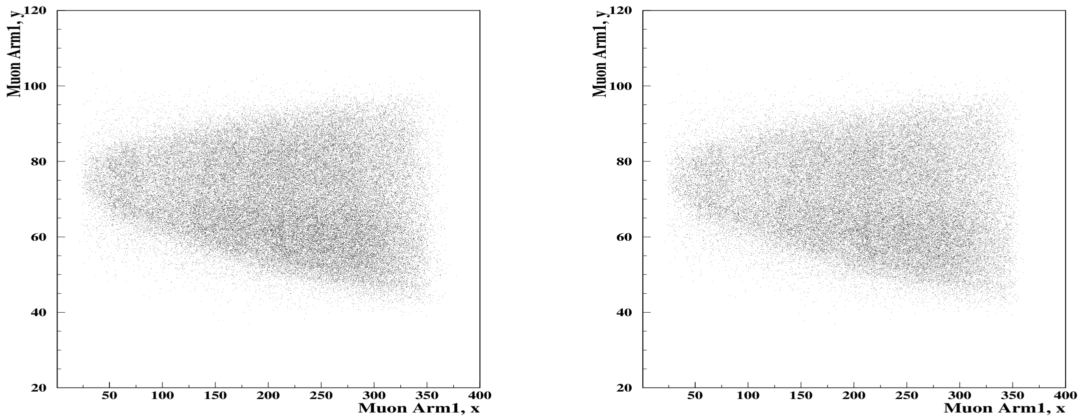

Figure 12: *Mu* x'_{tr} *vs* y'_{tr} *distributions before and after (left and right) muon finder procedure.*

Prsh ADC spectra could seem slightly different for μ and π as can be appreciated in figure 13 but the ratio between the ADC spectra does not confirm this hypothesis (see figure 14). So the interesting additional selection from *Prsh* could arrive only from *Prsh* time measurements.

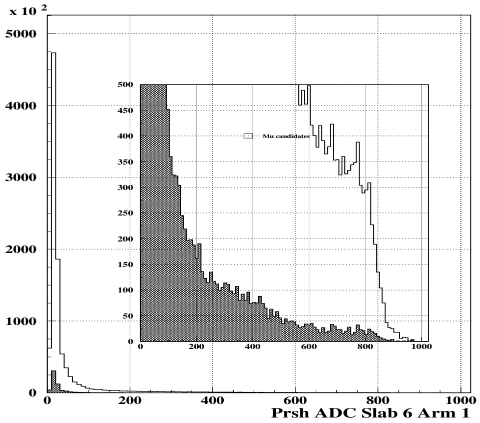

Figure 13: *ADC spectra for* μ *and* π *in Prsh slab 6 of Arm 1.*

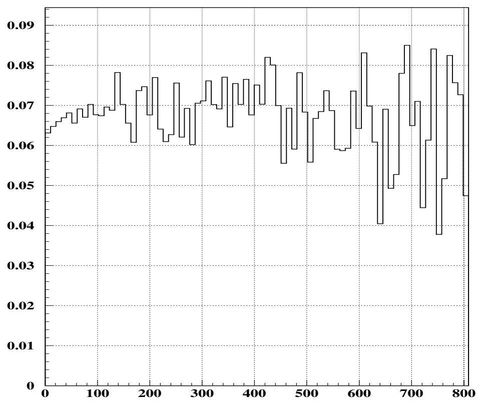

Figure 14: *ADC ratio for* μ *and* π *in Prsh slab 6 of Arm 1.*

In terms of momenta-spectra muon subtraction depends on track momentum as well as on arm. Muon subtraction is more important at low $|P|$ and for $|P| > 1.7GeV/c$ is also different for positive and negative particles. As can be expected proton contamination in Arm2 remains after muon subtraction and makes different momenta distributions in arms 1 and 2 for real events, but not for accidental events. Momentum of positive (Arm2) and negative (Arm1) particles for all $\pi\pi$ triggers and for selected muon events ($\mu\pi$, $\pi\mu$, $\mu\mu$) are displayed in figures 15 and 16.

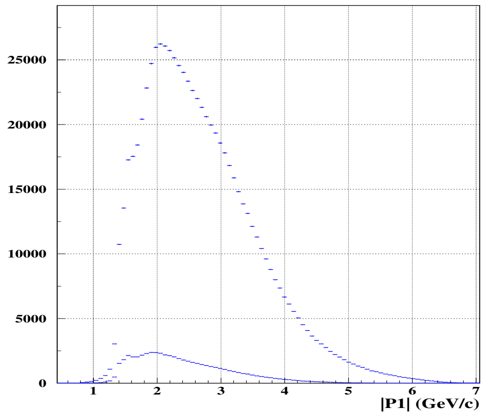

Figure 15: $|P|$ *distribution for all* $\pi\pi$ *triggers and for selected muon events* ($\mu\pi$, $\pi\mu$, $\mu\mu$) *in Arm1.*

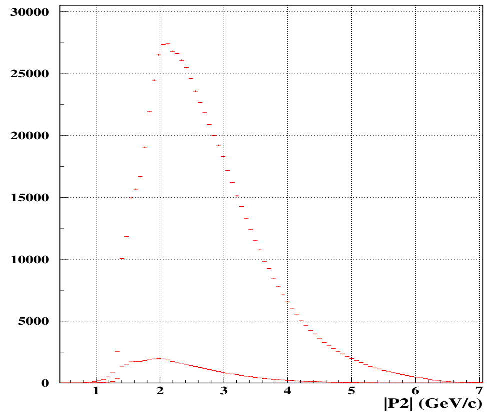

Figure 16: $|P|$ *distribution for all* $\pi\pi$ *triggers and for selected muon events* ($\mu\pi$, $\pi\mu$, $\mu\mu$) *in Arm2.*

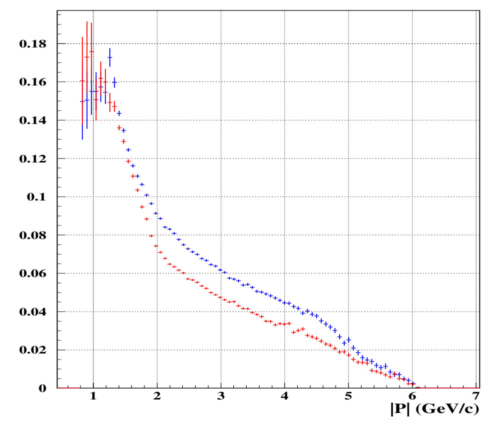

Figure 17: *Ratio* ($|P|$ *all* $\pi\pi$ *triggers*)/($|P|$ *muons events*) *distributions for Arm1 (blue-up) and Arm2 (red-down).*

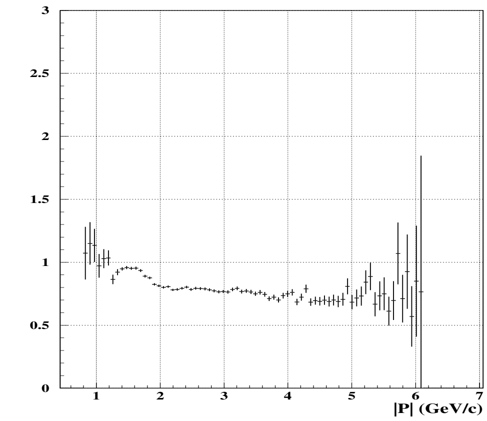

Figure 18: *Ratio of distributions in figure 17.*

Figure 17 shows differences between ratio distributions, $\frac{|P|\, for\, all\, \pi\pi\, triggers}{|P|\, muons}$, in both arms. The distribution at the top corresponds to negative particles (Arm1) and the other to positive particles (Arm 2). The proton contamination makes the difference for real but not for accidental events in which no differences are found as is shown in figures 19, 20, 21, 22. This can be understood looking at the plot $|P|$ versus time difference in VH, Δt for positive and negative tracks and taking into account that for real events $\Delta t \,\epsilon\, [-0.5, +0.5]$ and for accidental ones $\Delta t \,\epsilon\, [-15.0, -5.0]$ and $\Delta t \,\epsilon\, [+7.0, +17.0]$.

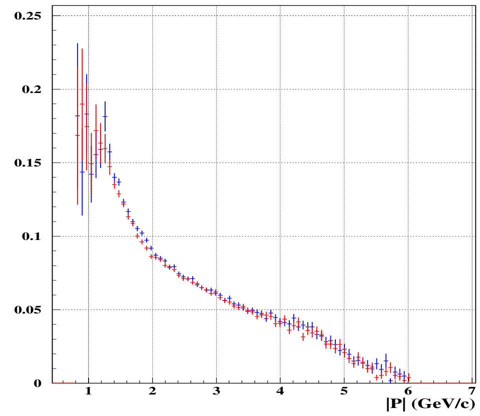

Figure 19: *Ratio (|P| all ππ triggers)/(|P| muon events) distributions in Arm1 (blue) and Arm2 (red) for accidental events.*

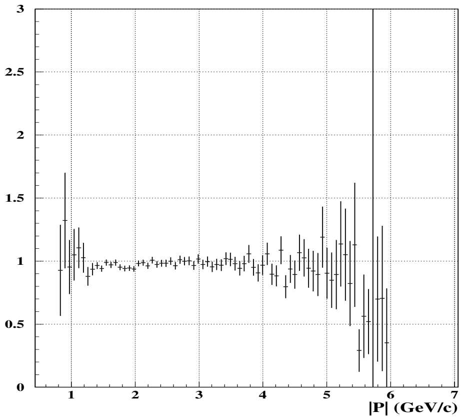

Figure 20: *Ratio of distributions in figure 19.*

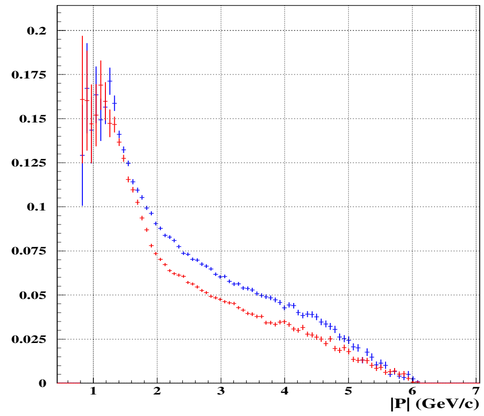

Figure 21: *Ratio (|P| all ππ triggers)/(|P| muon events) distributions in Arm1 (blue-up) and Arm2 (red-down) for accidental events.*

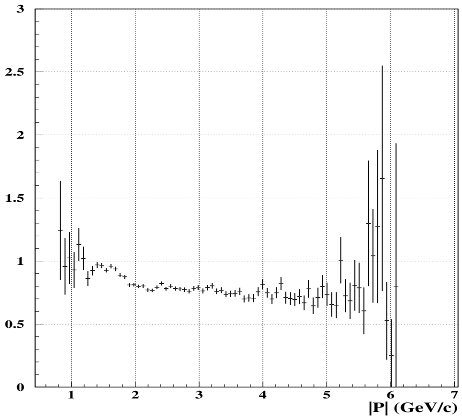

Figure 22: *Ratio of distributions in figure 21.*

Another item that must be studied is the muon subtraction effect in relative c.m.s. momentum, Q, distributions. DIRAC experiment is focused to events with very low relative momentum, and any cut in the on-line or off-line should be analyzed in terms of Q components distributions, Q_x, Q_y, Q_l; these distributions before and after muon subtraction and ratio between them are presented in figures 23-31 for all, real and accidental events. These distributions correspond to $1+1$ "good-pair" events and the Q values come from TmTrxDC common-block. The overall reduction of $\pi\pi$-trigger data is around $\sim 7\%$ and ratios between distributions before and after muon subtraction seem reasonable.

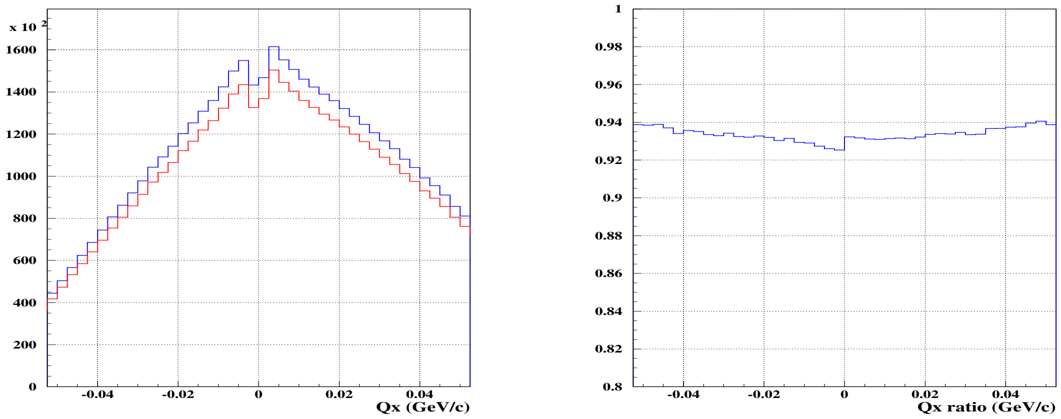

Figure 23: *Qx distributions before and after muon subtraction, and ratio between them for all time spectra.*

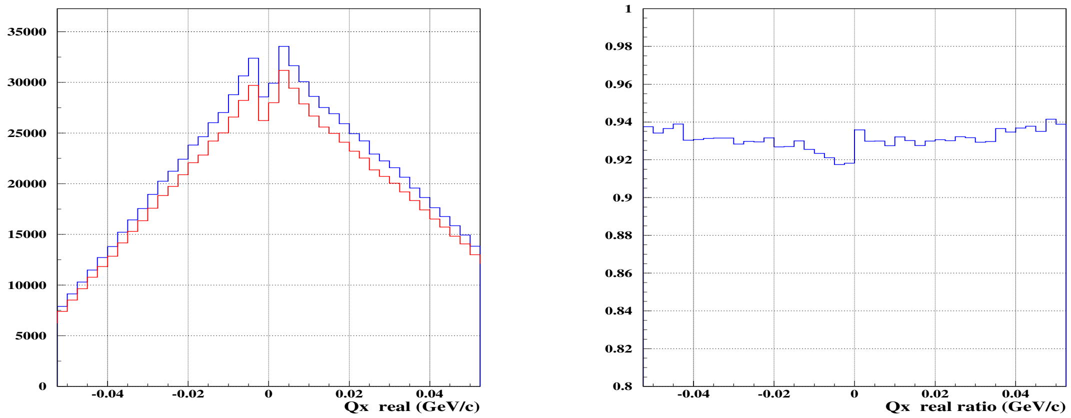

Figure 24: *Qx distributions before and after muon subtraction, and ratio between them for real events.*

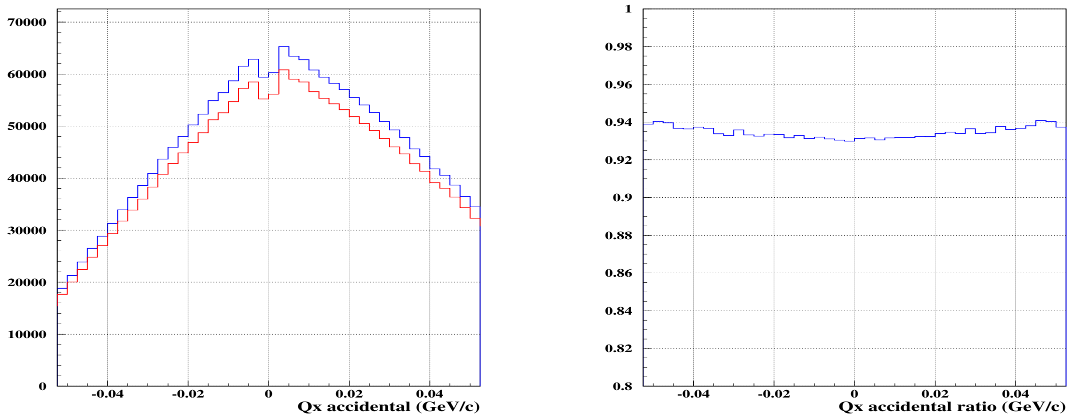

Figure 25: *Qx distributions before and after muon subtraction, and ratio between them for accidental events.*

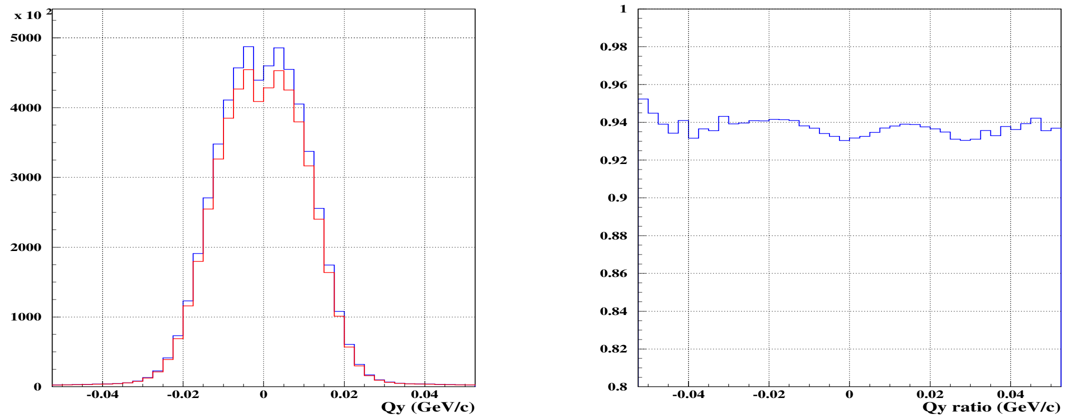

Figure 26: *Qy distributions before and after muon subtraction, and ratio between them for all time spectra.*

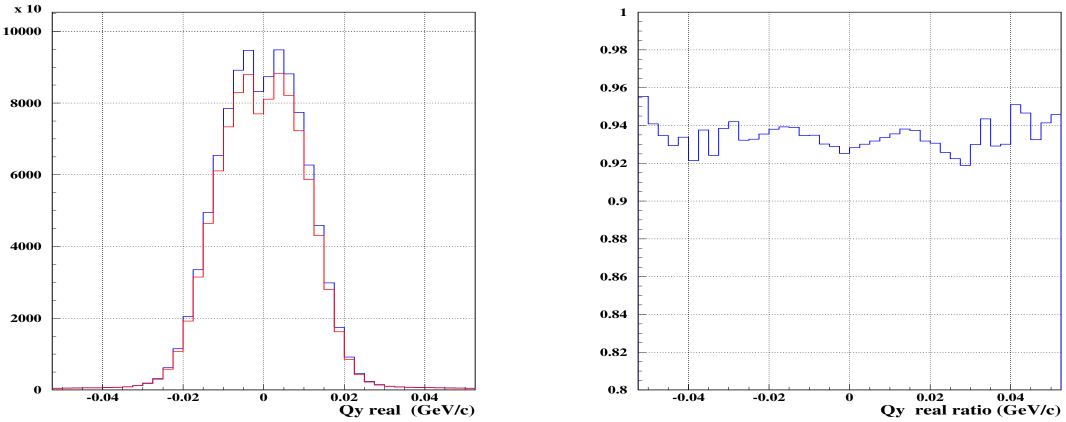

Figure 27: *Qy distributions before and after muon subtraction, and ratio between them for real events.*

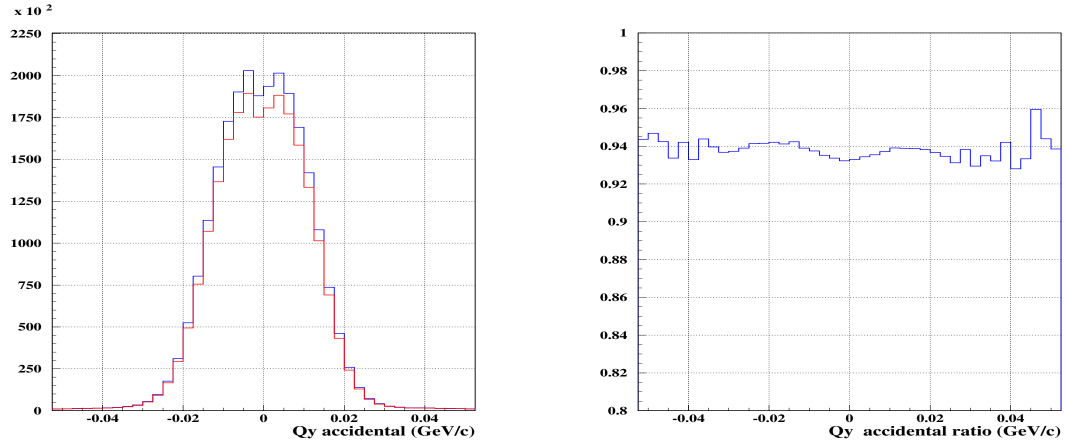

Figure 28: *Qy distributions before and after muon subtraction, and ratio between them for accidental events.*

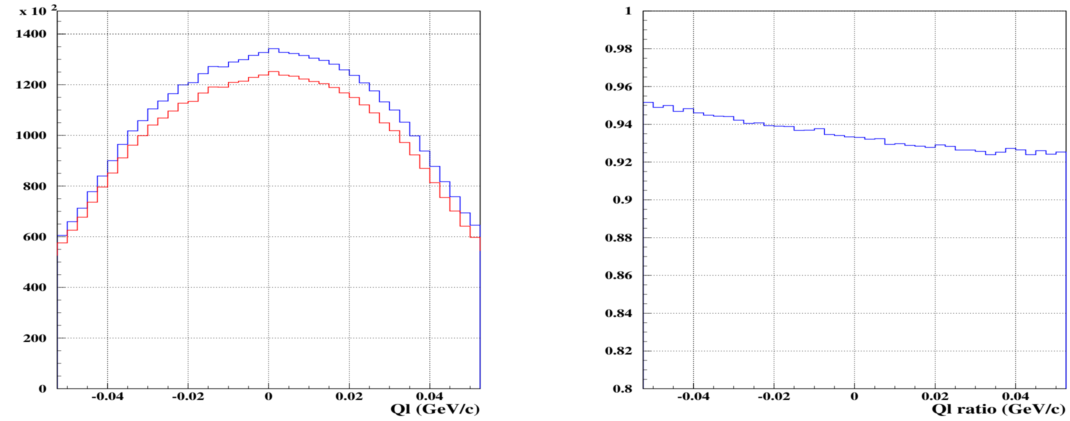

Figure 29: *Ql distributions before and after muon subtraction, and ratio between them for all time spectra.*

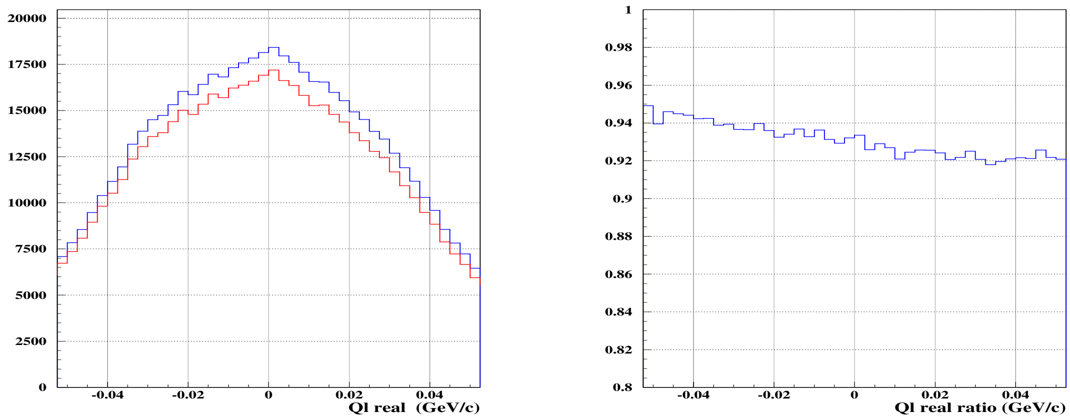

Figure 30: *Ql distributions before and after muon subtraction, and ratio between them for real events.*

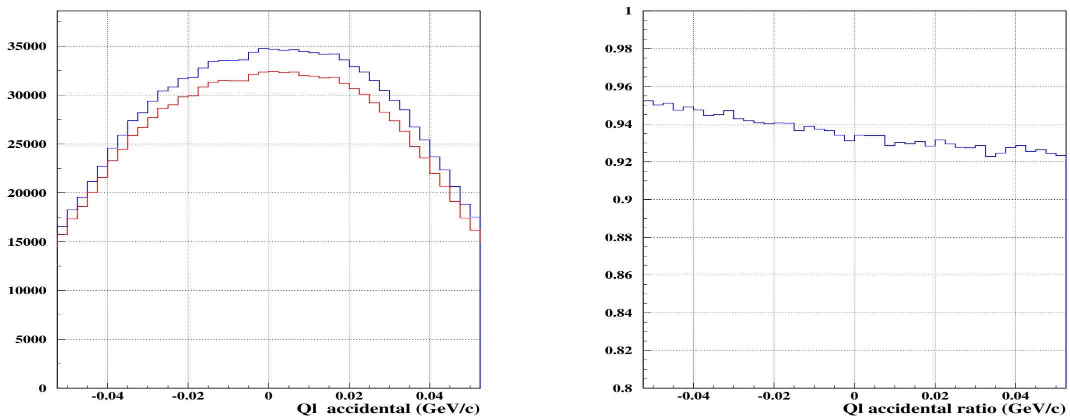

Figure 31: *Ql distributions before and after muon subtraction, and ratio between them for accidental events.*

5 Conclusions

A procedure for muon identification has been developed and it is available in standard ARIANE. The "muon signal" criteria can be easily modify in the FFReadInput file and with the proposed cuts for "muon signal" definition ($DtwindowMusignal = 5\,ns$, $DxwindowMusignal = 18\,cm$) the data reduction is $\sim 7\%$. The lost of pion events could be estimated in $2-3\,\%$ of the rejected muons due to Mu detector design and $3-4\,\%$ due to background and false muon identification.

References

[1] B.Adeva et al., Lifetime measurement of $\pi^+\pi^-$ atoms to test low energy QCD predictions, (Proposal to the SPSLC, CERN/SPSLC 95–1, SPSLC/P 284, Geneva 1995)

[2] V. Brekhovskikh, "Status of Muon Detector",DIRAC collaboration meeting, June 2000.

[3] V. Brekhovskikh, M. Gallas, "The μ-identification", DIRAC collaboration meeting, November 2000.